ACS APPLIED MATERIALS & INTERFACES

www.acsami.org

Research Article

On-Demand Local Immunomodulation via Epigenetic Control of Macrophages Using an Inflammation-Responsive Hydrogel for Accelerated Wound Healing

Hyerim Kim, Yunji Joo, Yun-Min Kook, Na Ly Tran, Sang-Heon Kim, Kangwon Lee,* and Seung Ja Oh*

Cite This: https://doi.org/10.1021/acsami.1c20394

Read Online

ACCESS | Metrics & More | Article Recommendations | Supporting Information

ABSTRACT: Effective resolution of inflammation contributes to favorable tissue regenerative therapeutic outcomes. However, fine coordination of local immunomodulation in a timely manner is limited because of the lack of strategies for controlling disease dynamics. We developed an inflammation-responsive hydrogel (IFRep gel) as an effective therapeutic strategy for on-demand epigenetic modulation against disease dynamics in wound healing. The IFRep gel is designed to control drug release by cathepsins according to the state of inflammation for active disease treatment. The gel loaded with an inhibitor of the epigenetic reader bromodomain (BRD)4 regulates the translocation of nuclear factor erythroid 2 to the nucleus, where it promotes antioxidant gene expression to reverse the inflammatory macrophage state *in vitro*. In addition, on-demand BRD inhibition using the responsive hydrogel accelerates wound healing by controlling the early inflammatory phase and keratinocyte activation *in vivo*. Our data demonstrate the clinical utility of using the IFRep gel as a promising strategy for improving therapeutic outcomes in inflammation-associated diseases.

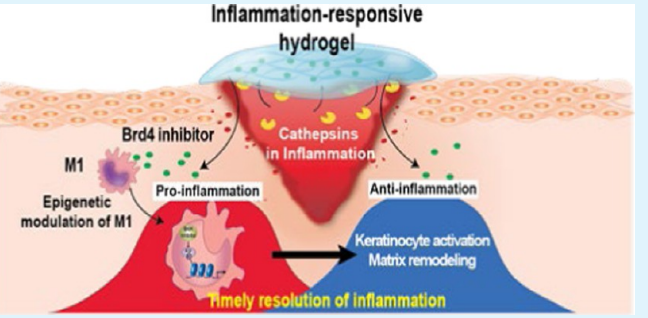

KEYWORDS: *inflammation-responsive hydrogel, drug release, anti-inflammation, epigenetic modulation, macrophage, wound healing*

INTRODUCTION

An inflammatory response is essential for healing and is the first response following tissue damage. Effective resolution of inflammation contributes to the prevention of disease progression and acceleration of healing.[1,2] Therefore, methods for resolving inflammation are regarded as promising strategies for the successful healing and tissue regeneration.[3,4] Biomaterial-based hydrogels have been used as anti-inflammatory factor carriers for local immunomodulation.[5] Many research groups have studied diverse hydrogels such as gelatin methacryloyl,[6] alginate,[7] chitosan,[8] and polyethylene glycol[9] to deliver anti-inflammatory molecules for anti-inflammation therapy in the wound healing process. For example, Saleh et al. used microRNA-loaded adhesive gelatin methacryloyl hydrogel for local and targeted delivery of microRNA, which accelerated wound healing by inducing M2 anti-inflammatory macrophages at the wound site.[6] Moreover, Salehi et al. demonstrated effective anti-inflammation and wound healing using sustained release of anti-inflammatory molecules from alginate hydrogel.[7] However, passive drug delivery using nonresponsive hydrogels has a limited capacity to actively resolve inflammation. Although various hydrogels that respond to the inflammatory environment, such as those sensitive to pH,[10,11] reactive oxygen species,[10] and matrix metalloproteinases,[12−14] have been developed for effective inflammation regulation, the temporal resolution of inflammation essential for tissue regeneration remains challenging.[15,16]

During the wound healing process, the plasticity of macrophages, i.e., M1−M2 transition, is a key factor controlling the switch from an acute inflammatory response to the resolution phase of the inflammatory process. M1 macrophages are highly phagocytic cells capable of removing debris, whereas M2 macrophages promote regeneration by inducing matrix remodeling.[17] Epigenetic modulation is an effective strategy for changing the phenotype of macrophages because of its strong efficacy, target specificity, and reversibility in controlling macrophage plasticity.[18,19] Recent studies demonstrated that a bromodomain (BRD) inhibitor, as an epigenetic drug, effectively modulated the plasticity of

Received: October 22, 2021
Accepted: December 28, 2021

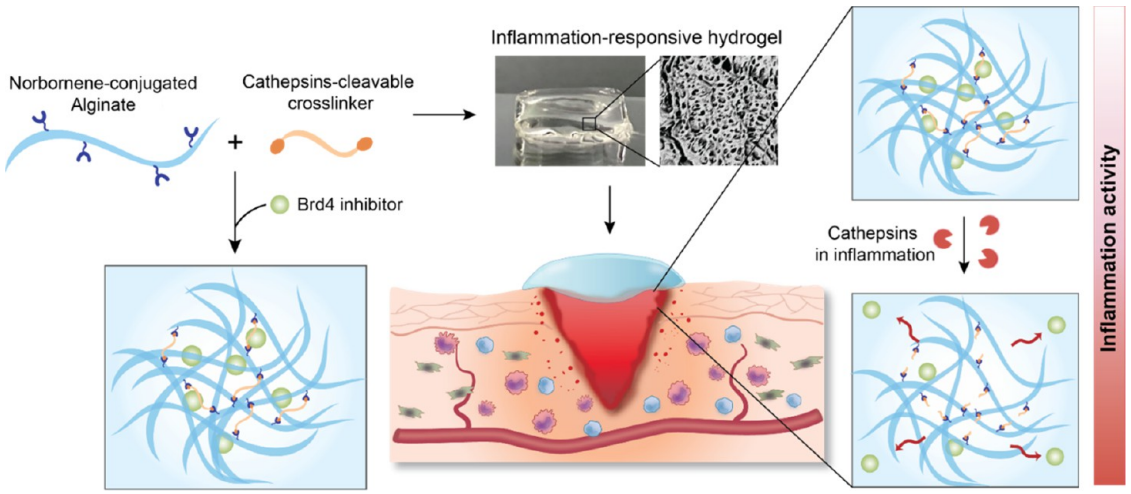

Figure 1. Schematic illustration of inflammation-responsive hydrogel (IFRep gel) for local immunomodulation. IFRep gel is formed with cross-linking between the Norbornene-conjugated alginate and cathepsins-cleavable cross-linker. The BRD4 inhibitor-loaded IFRep gels respond to cathepsins overexpressed in inflammation environment and resolve the inflammation via actively released BRD4 inhibitor from the IFRep gel.

inflammatory macrophages.[20,21] Therefore, alleviating the inflammatory response through epigenetic modulation of macrophages may be a useful therapeutic strategy in clinical applications. However, as epigenetic drugs have a very short half-life and the epigenome is sensitively regulated according to the environment, it is important to minimize the off-target effects of epigenetic drugs.[22] Most studies of the delivery of epigenetic drugs have focused on nanocarriers, which cannot deliver drugs in an on-demand manner and exhibit toxic side effects following accumulation in the liver or spleen by the circulation system after injection.[23] Therefore, a local and spatiotemporal drug delivery system is needed to control inflammation through effective epigenetic modulation of macrophages.

In this study, we developed an inflammation-responsive hydrogel (IFRep gel) capable of on-demand epigenetic modulation in response to inflammation activity, resulting in accelerated wound healing. *In vitro* and *in vivo* screening revealed that cathepsins L, S, and B are representative enzymes reflecting inflammatory activity. To enable controlled drug release by enzymes consistent with the inflammatory state, an IFRep gel was prepared using norbornene-modified alginate cross-linked with cathepsins-cleavable peptides via thiol-ene click chemistry. The precise programmability of IFRep gel enabled the BRD4 inhibitor to control inflammation and keratinocyte activation at a specific time, resulting in accelerated wound healing *in vivo*. Therefore, the IFRep gel capable of on-demand BRD4 inhibition is a promising therapeutic strategy targeting epigenetics for favorable immunomodulation in treating different types of inflammatory diseases using different combinations of drugs.

RESULTS AND DISCUSSION

IFRep Gel Controlling Drug Release According to the State of Disease. Treatment according to the disease state contributes to efficient therapeutic outcomes and was achieved by our IFRep gel. By cross-linking with cathepsins-cleavable peptides, the hydrogel facilitated disassembly and drug release in response to enzymatic activities reflecting the disease state (Figure 1). The IFRep gel loaded with an inhibitor of the epigenetic reader BRD4 regulated the translocation of nuclear factor erythroid 2 (Nrf2) to the nucleus, where it promoted antioxidant gene expression to reverse the inflammatory macrophage state *in vitro*. In addition, on-demand BRD4 inhibition using the responsive hydrogel accelerated wound healing through timely control of the inflammatory phase and keratinocyte activation *in vivo*.

Enhanced Expression of Cathepsins in Acute Inflammation after Injury. Among the various immune cells involved in inflammation, macrophages play critical roles in each stage of the healing process. To screen representative biomarkers reflecting inflammation, we first tested THP-1-driven M1 macrophages to assess whether enzyme expression was enhanced. The mRNA expression of diverse cathepsins was enhanced in M1-like macrophage (Figure 2a), also the cathepsin protein levels in conditioned media of M1-like macrophages were higher compared to in those of M0 macrophages (Figure 2b).

Moreover, we confirmed the enhanced enzymatic activity of cathepsins L, S, and B among the overexpressed enzymes, indicating that these enzymes secreted from inflammatory M1 macrophages contribute to the acute inflammatory response following injury (Figure 2c).

To observe the correlation between the expression level of cathepsins and inflammation state, we created wound injuries using an 8 mm full-thickness biopsy punch on the dorsal skin of Balb/c mice. The mRNA level of inflammatory markers, such as tumor necrosis factor (TNF)-α, inducible nitric oxide synthase (iNOS), and interleukin 1β (IL1β), was significantly increased on days 2 and 5 after injury (Figure 2d). Interestingly, quantitative PCR revealed enhanced expression of cathepsins L, S, and B, with the same increasing tendency as that observed with inflammatory markers following injury (Figure 2e). Immunofluorescence staining of damaged tissue showed enhanced iNOS and TNF-α expression with increasing M1 macrophage populations (CD11b + iNOS+ positive cells) after injury (Figure 2f,h); these results are consistent with those of mRNA expression analysis. Increased expression of cathepsins L, S, and B was confirmed at the protein level (Figure 2g,i). Together, the results indicated that cathepsins L, S, and B secreted by inflammatory M1 macrophages are representative biomarkers of acute inflammation activity in injury.[24,25]

https://doi.org/10.1021/acsami.1c20394
ACS Appl. Mater. Interfaces XXXX, XXX, XXX−XXX

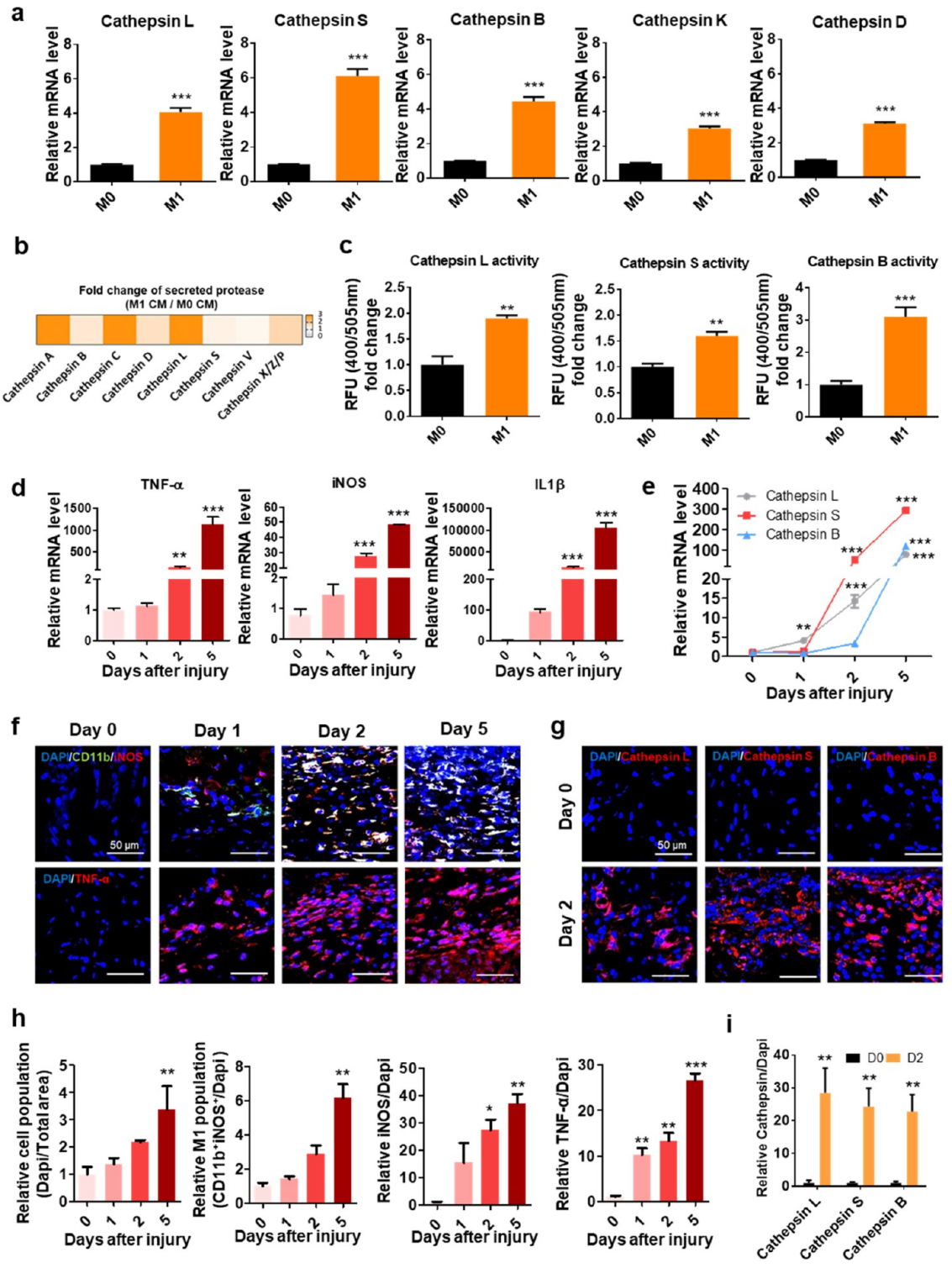

Figure 2. Overexpression of cathepsins in inflammation after injury *in vivo* and *in vitro*. (a) mRNA level of various cathepsins in M0- and M1-like macrophages. (b) Diverse cathepsins expression array in M0- and M1-like macrophages conditioned media. (c) Cathepsins activity in M0- and M1-like macrophages. (d) mRNA expression level of inflammatory markers on days 0, 1, 2, and 5 after wound injury *in vivo*. (e) mRNA level of cathepsins L, S, and B at different time points after injury. (f) Immunofluorescence staining of CD11b (macrophage, green), iNOS, and TNF-α (inflammatory markers, red) at days after injury. (g) Cathepsins L, S, and B immunofluorescence staining for injury site on day 2. (h) Quantification of increased cell population and M1 macrophage population days after injury. Also, quantification of stained inflammatory markers and (i) cathepsins in immunofluorescence images.

Development and Characterization of IFRep Gel. To test active inflammatory modulation via epigenetic regulation to achieve desired therapeutic outcomes, the IFRep gel was designed to control drug release by cathepsins according to the inflammation state. To prepare the IFRep gel, biocompatible and deformable alginates were used to prepare cathepsins-cleavable hydrogels. The carboxylic groups of alginate were conjugated with norbornene via a 1-ethyl-3-(3-

https://doi.org/10.1021/acsami.1c20394
ACS Appl. Mater. Interfaces XXXX, XXX, XXX−XXX

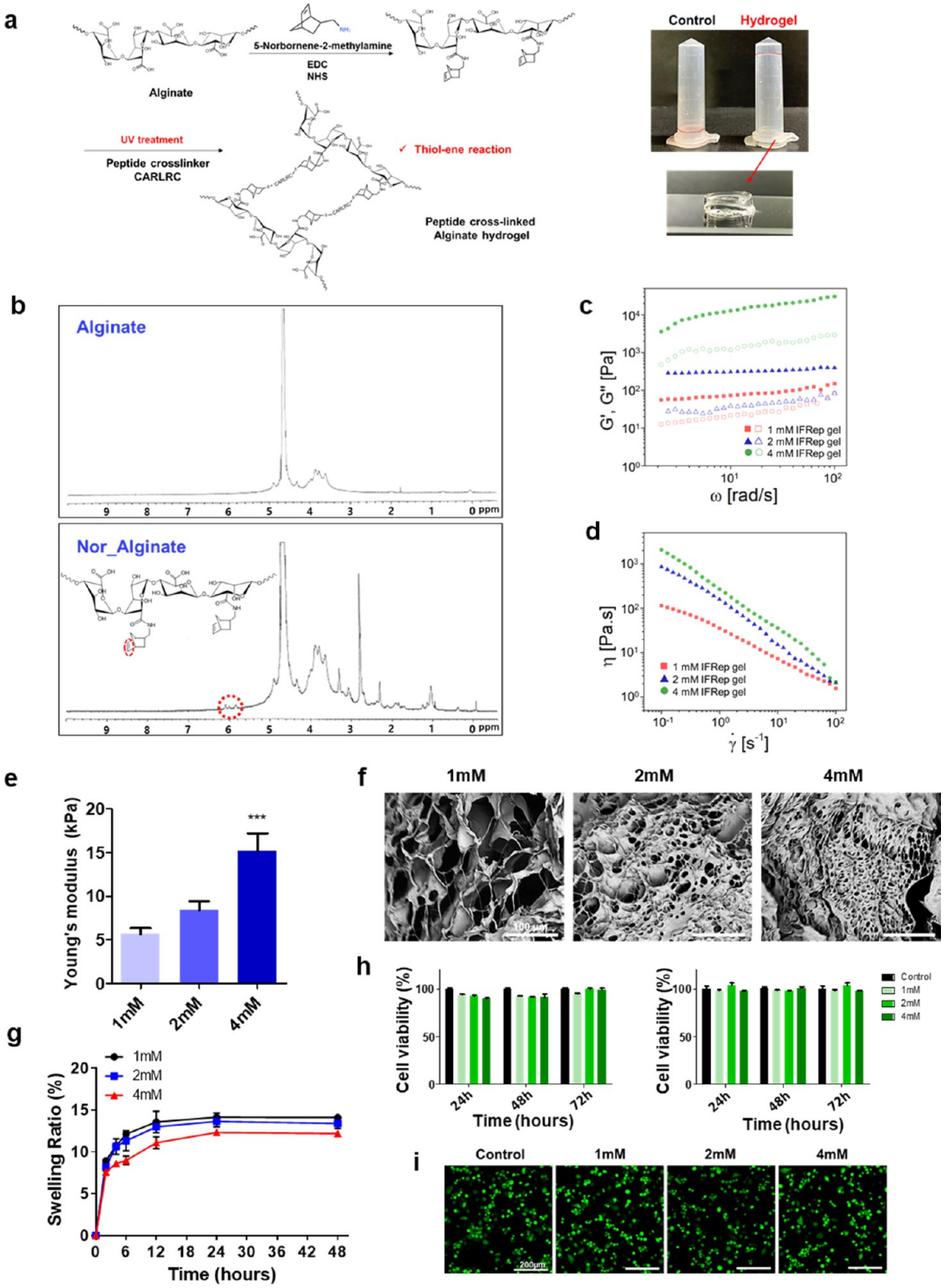

Figure 3. Characterization of the inflammation-responsive hydrogel. (a) Fabrication of inflammation-responsive alginate hydrogel. (b) Chemical composition analysis by ^{1}H-NMR. (c) Storage modulus (G', full dots) and loss modulus (G'', empty dots) in different concentrations of peptide cross-linked hydrogels. (d) Viscosity (η) as a function of shear rates for different concentrations of peptide cross-linked hydrogels. (e) Stiffness of hydrogels via Young's modulus value (mean ± SD, n = 3), ***p < 0.001. (f) Scanning electron microscopy (SEM) images for hydrogel network. (g) Swelling ratio (%) of hydrogels (mean ± SD, n = 3). (h) Cell viability (%) of fibroblasts and macrophages when cultured with hydrogels (mean ± SD, n = 3). (i) Live and dead cell staining after 72 h cultured with hydrogels.

dimethylaminopropyl)carbodiimide/*N*-hydroxysuccinimide (EDC/NHS) synthesis method for photoinitiative click chemistry with a cathepsins-cleavable peptide cross-linker (Figure 3a). Successful conjugation of norbornene with alginate was confirmed using ^{1}H-NMR (Figure 3b). Consistent with previous studies, double bonds of norbornene groups

https://doi.org/10.1021/acsami.1c20394
ACS Appl. Mater. Interfaces XXXX, XXX, XXX−XXX

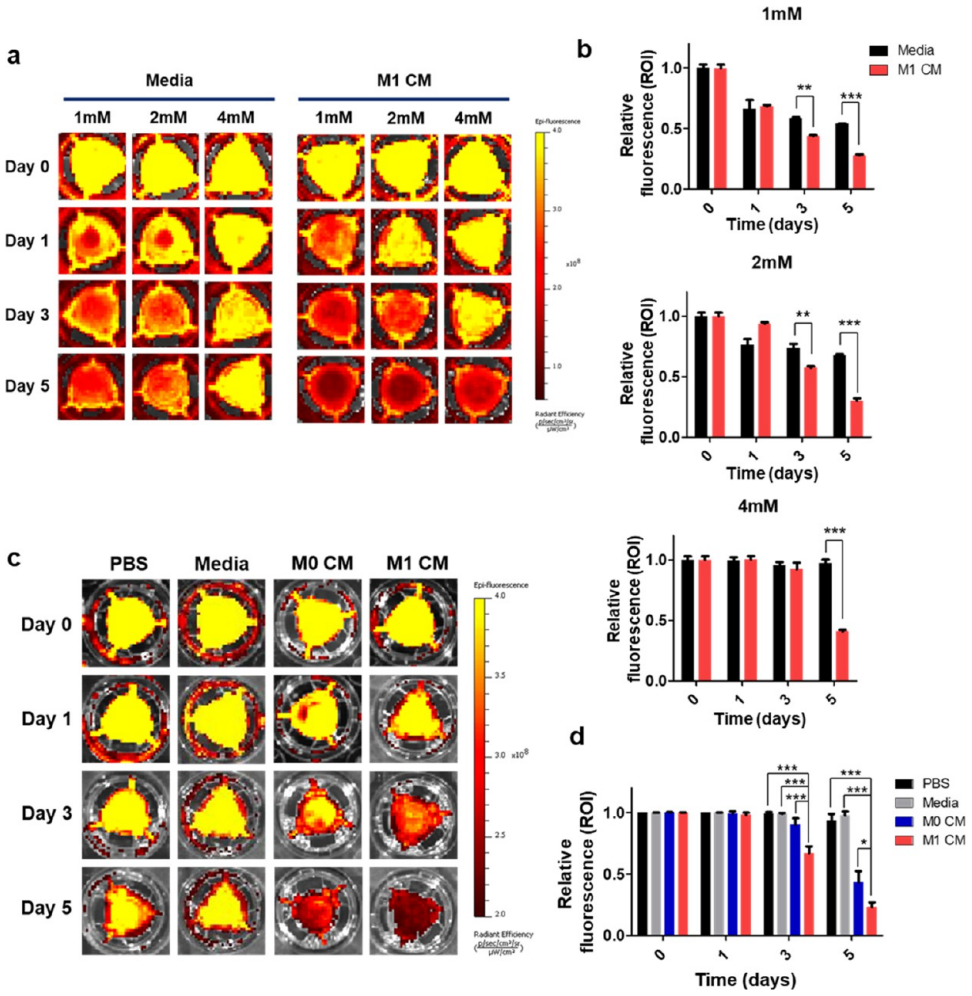

Figure 4. Control of responsiveness of inflammation-responsive hydrogel. (a) Hydrogel sensitivity to the conditioned media of M1-like macrophage depending on peptide cross-linker concentration was imaged by *in vivo* imaging system (IVIS). (b) Relative fluorescence intensity curve (mean ± SD, $n = 3$), $^{**}p < 0.01$, $^{***}p < 0.001$. (c) Dextran-loaded IFRep gel was incubated in PBS, media, M0-, and M1-like macrophage-conditioned media and imaged by IVIS. (d) Relative fluorescence curve of remained dextran fluorescence intensity at each time point (mean ± SD, $n = 3$), $^{*}p < 0.1$, $^{***}p < 0.001$.

were detected at 6.2−5.8 ppm, demonstrating successful conjugation of norbornene to alginate;[26−28] norbornene-conjugated alginate (Nor-Alginate) was made in a gel form via thiol-ene cross-linking between the thiol group of a cathepsins-cleavable cross-linker and norbornene by exposure to UV light.[26,29]

To analyze the mechanical properties of the IFRep gel, storage modulus (G') and loss modulus (G'') were assessed using oscillatory shear rheology. The storage modulus (indicating the elastic property) and loss modulus (indicating the viscous property) were measured under oscillatory frequency. G' was higher than G'' at all concentrations of cathepsins-cleavable cross-linker groups. As the concentration of cathepsins-cleavable cross-linker increased, the G′ value increased (Figure 3c), indicating a higher elastic property, and the viscosity of the hydrogel also increased (Figure 3d). Moreover, Young's modulus values revealed higher stiffness with increasing concentrations of the cathepsins-cleavable cross-linker (Figure 3e). The increased mechanical property was correlated with an increased network density, as measured using scanning electron microscopy (SEM) (Figure 3f). Additionally, the network density of the IFRep gel was related to its swelling properties. The swelling behavior of the IFRep gels was measured by assessing the weight after incubation in phosphate-buffered saline (PBS; pH 7.4). The swelling rate gradually increased over 48 h, and the equilibrium was accelerated as the cathepsins-cleavable cross-linker concentration decreased. These results indicate that the swelling rate increased as the peptide cross-linking decreased (Figure 3g). Moreover, the IFRep gel made of various concentrations of cathepsins-cleavable cross-linker did not affect fibroblast and macrophage viability, indicating that the hydrogel is biocompatible (Figure 3h,i).

Function of IFRep Gel and Optimization for Drug Release. To confirm the disassembly and drug release by the IFRep gel in response to cathepsin activity, IFRep gels with different cross-linker concentrations were evaluated. Dextran, a fluorescent dye, was loaded in the IFRep gels and immersed in the control and conditioned media of M1-like macrophages. The reduced fluorescence of IFRep gels was monitored using an *in vivo* imaging system (IVIS) (Figure 4a,b). At cross-linker concentrations of 1 and 2 mM in the IFRep gel, the dye was released in the control medium starting on day 1, and the release rate was accelerated following exposure to the conditioned medium. However, IFRep gels with a cross-linker concentration of 4 mM exhibited stable behavior in the control

https://doi.org/10.1021/acsami.1c20394
ACS Appl. Mater. Interfaces XXXX, XXX, XXX−XXX

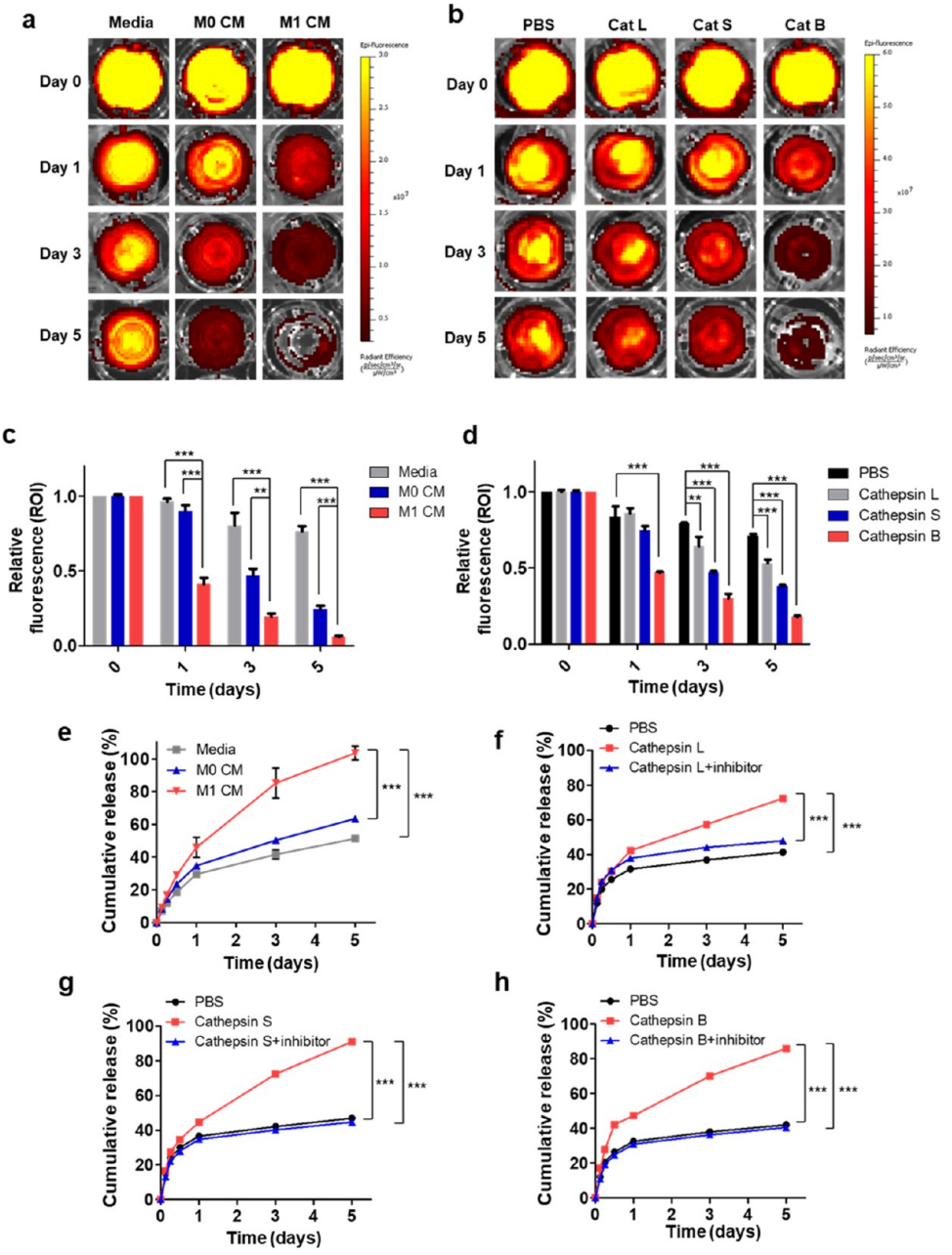

Figure 5. Small-molecule release amplified in response to the environment. (a) Cy7-CA-loaded IFRep gel was incubated in nonactivated and activated macrophage-conditioned media and imaged by IVIS. (b) Cy7-CA-loaded IFRep was incubated in PBS with cathepsins L, S, and B, respectively, and imaged by IVIS. (c, d) Relative fluorescence intensity curve of remained Cy7-CA fluorescence at each time point. (e) JQ1 cumulative release profile from IFRep gel in M0- and M1-like macrophage-conditioned media (mean ± SD, $n = 3$), ***$p < 0.001$. (f–h) *In vitro* release kinetics of JQ1 from IFRep gel in PBS at 37 °C with cathepsins L, S, B, and cathepsins inhibitor (mean ± SD, $n = 4$), ***$p < 0.001$.

medium and started releasing the dye in the conditioned medium starting on day 3, indicating a tighter hydrogel network compared to that with 1 and 2 mM concentration of cross-linked IFRep gels. The difference in fluorescence of the IFRep gel between the control and conditioned media increased as the concentration of the cross-linker increased. Therefore, we selected the IFRep gel with a 4 mM cross-linker with an appropriate network density for further studies. The dextran-loaded IFRep gel was exposed to different conditions, such as PBS, control media, and conditioned media, for M0- and M1-like macrophages (Figure 4c,d). The fluorescence intensity was stable in PBS and the media groups but responsive in M0- and M1-conditioned media during the study period. The IFRep gel exhibited the highest dye release in M1-conditioned media.

To observe the small-molecule release profile of IFRep gels, the fluorescent dye Cy7-CA, a model compound of small molecules,[30] was loaded into the IFRep gels. The gels were exposed to various conditions. Dextran was not released from the IFRep gel when exposed to the control medium lacking cathepsins, whereas 20% of the initial loading amount of Cy7-CA was released (Figure 5a,c). The release rate of Cy7-CA was accelerated when the Cy7-CA-loaded IFRep gel was exposed to M0- and M1-conditioned media, releasing approximately 100% of the loaded amount following exposure to M1-conditioned medium.

https://doi.org/10.1021/acsami.1c20394
ACS Appl. Mater. Interfaces XXXX, XXX, XXX−XXX

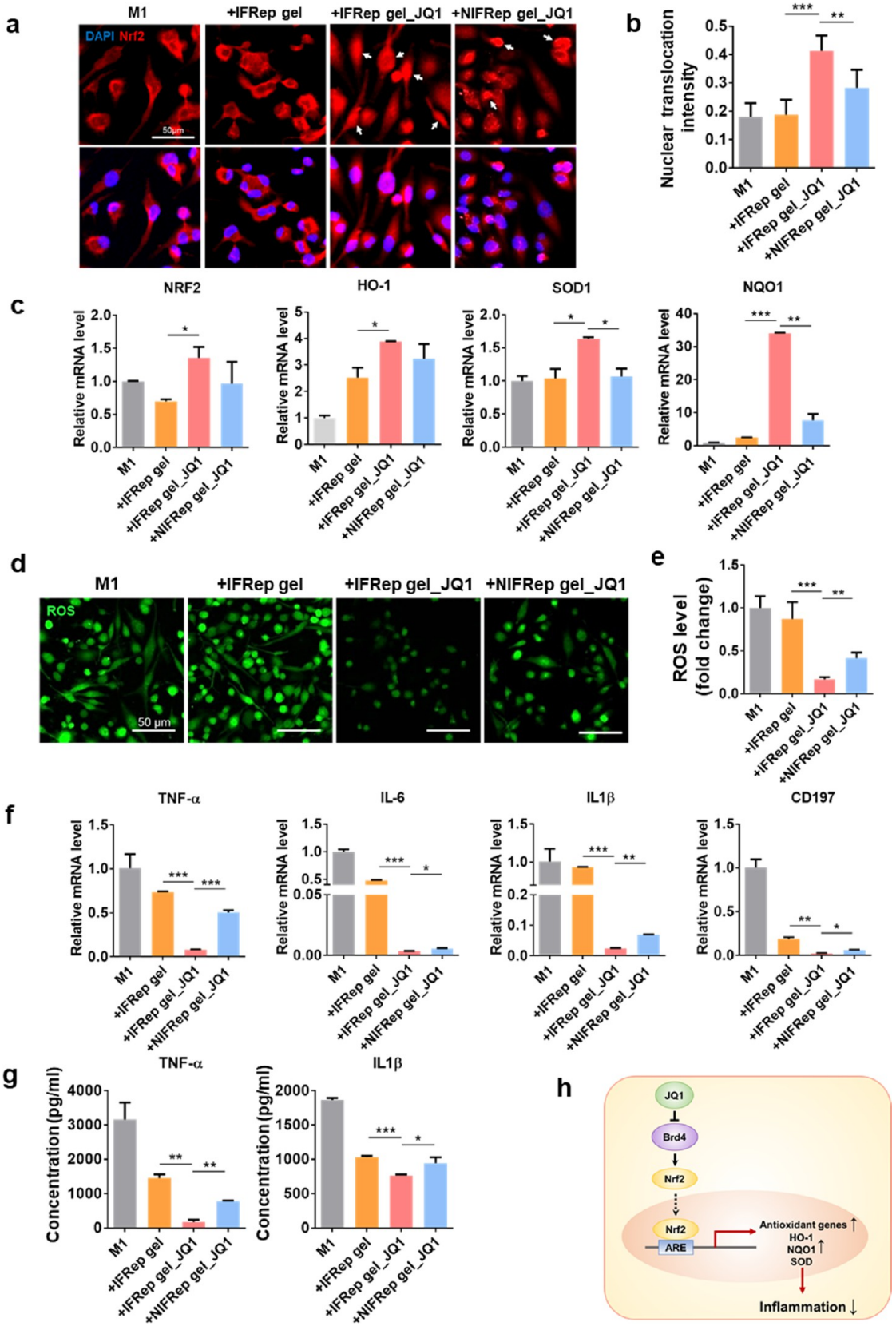

Figure 6. JQ1-loaded inflammation-responsive hydrogel for anti-inflammation effect via epigenetic modification. (a) Nrf2 immunofluorescence image of M1-like macrophage after 48 h incubation with IFRep gel, JQ1-loaded IFRep gel, and JQ1-loaded NIFRep gel. (b) Nuclear translocation intensity of Nrf2. (c) mRNA level of Nrf2 and antioxidant genes. (d) Reactive oxygen species (ROS) fluorescence staining of M1-like macrophages and (e) quantification of ROS fluorescence intensity. (f) mRNA level of inflammatory markers in M1-like macrophage. (g) ELISA analysis of TNF-α and IL-1β in conditioned media of M1-like macrophages. (h) Schematic illustration of signaling pathways of BRD4 inhibitor effects on anti-inflammation via epigenetic regulation. Data are presented as mean ± SD, $n = 3$ (*$p < 0.1$, **$p < 0.01$, ***$p < 0.001$).

https://doi.org/10.1021/acsami.1c20394
ACS Appl. Mater. Interfaces XXXX, XXX, XXX−XXX

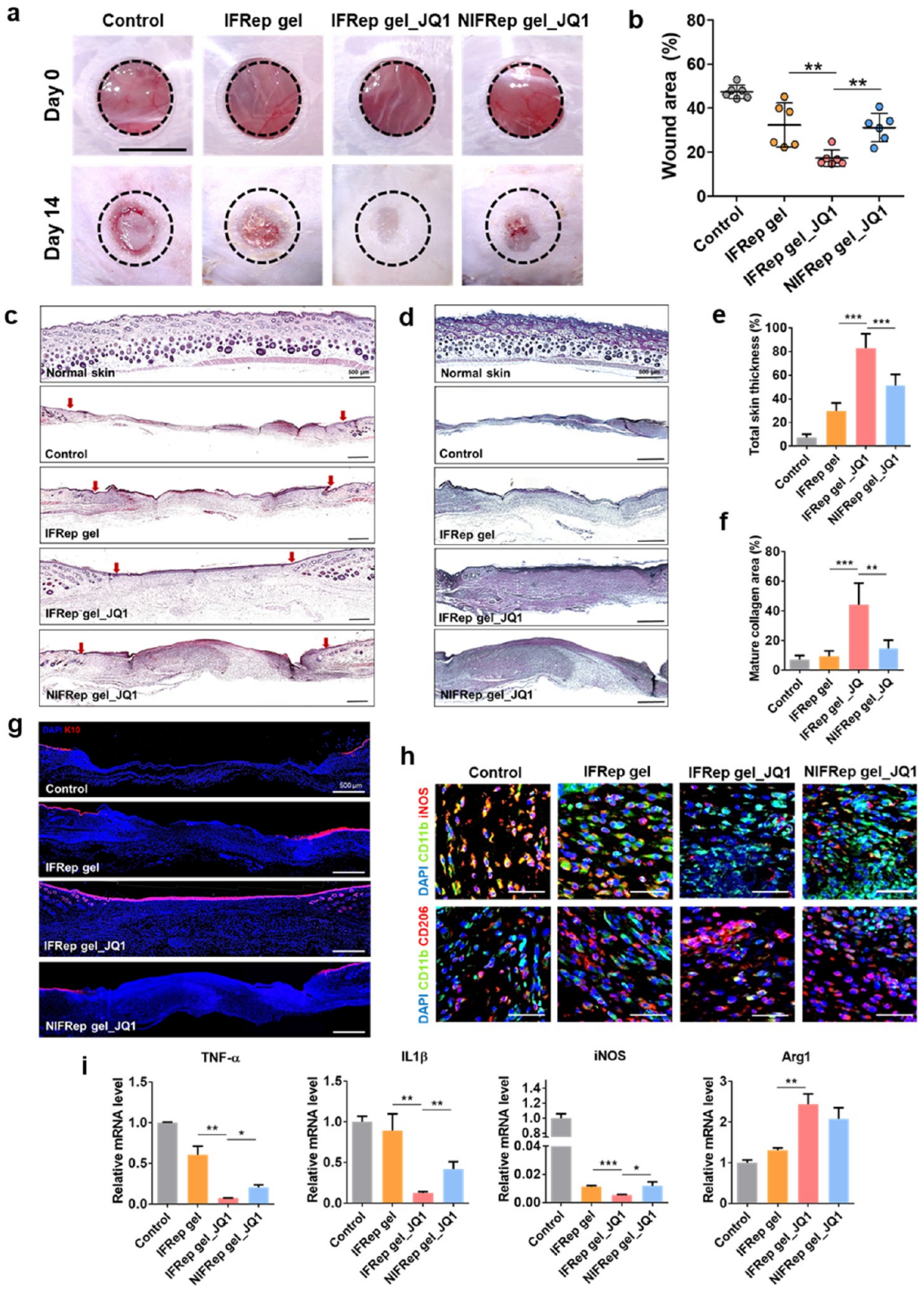

Figure 7. BRD4 inhibitor-loaded inflammation-responsive hydrogel-accelerated wound healing *in vivo*. (a) Representative images of wound closure after 14 days treated with JQ1-loaded hydrogels (mean ± SD, $n = 6$), $^{**}p < 0.01$. (b) Wound closure rate (%) after 14 days. (c) H&E staining of wound section at day 14. (d) Herovici staining of wound section on day 14. (e) Regenerated dermal thickness after 14 days normalized by normal skin tissue thickness in H&E stained images (mean ± SD, $n = 4$), $^{***}p < 0.001$. (f) Mature collagen area in wound area of Herovici stained images (mean ± SD, $n = 4$), $^{**}p < 0.01$, $^{***}p < 0.001$. (g) Immunofluorescence staining of cytokeratin 10 in all groups on day 14. (h) Immunofluorescence staining of M1 (CD11b+ iNOS+) and M2 (CD11b+ CD206+) markers on day 14. (i) Relative mRNA level of inflammatory and anti-inflammatory markers (mean ± SD, $n = 3$), $^{*}p < 0.1$, $^{**}p < 0.01$, $^{***}p < 0.001$.

https://doi.org/10.1021/acsami.1c20394
ACS Appl. Mater. Interfaces XXXX, XXX, XXX−XXX

Furthermore, Cy7-CA-loaded IFRep gels were incubated in PBS (pH 7.4) with or without cathepsins L, S, and B (100 ng/mL) at 37 °C. Cathepsins triggered cleavage of the cross-linker, accelerating the release of loaded Cy7-CA (Figure 5b,d). The rate of Cy7-CA release was faster in the order of cathepsins B, S, and L, indicating a priority of cleavage based on the type of cathepsin.

The drug release profile of JQ1, an inhibitor of the epigenetic reader BRD4, was evaluated by assessing UV absorbance under various conditions. JQ1-loaded IFRep gels were incubated in the control and M0- and M1-like macrophage-conditioned media at 37 °C (Figure 5e). M1-conditioned media under an inflammation-like environment led to the intense release of JQ1, whereas no significant release was observed in M0-conditioned media compared to that in the control media. Additionally, JQ1-loaded IFRep gels were incubated in PBS with cathepsins L, S, and B (100 ng/mL) with or without cathepsin inhibitor (Figure 5f–h). Cathepsins induced an increase in cumulative drug release; in contrast, the addition of a cathepsin inhibitor suppressed drug release, resulting in a profile similar to that after exposure to PBS. Moreover, as observed in the Cy7-CA release study, the cumulative release of JQ1 was lower for cathepsin L than for cathepsins S and B, although no significant difference was observed between the release profiles of cathepsins S and B.

Inhibition of Inflammatory Macrophage Responses via IFRep Gel Loaded with a BRD4 Inhibitor. Epigenetic modulation has been proposed as a potential therapeutic strategy in various diseases.[31] As the response of epigenetic machinery against environmental stimuli is highly sensitive, proper regulation of epigenetics according to the disease state is critical.[17] On-demand epigenetic control of inflammation could be a favorable approach for achieving safe and effective therapeutic outcomes in tissue regeneration because of its reversibility and target specificity. To confer the ability of on-demand epigenetic control against inflammation activity to the IFRep gel, we loaded a BRD4 inhibitor JQ1, which is responsible for histone modification, in the gel. To test the effect of BRD4 inhibition on inflammation, we first tested the expression of TNF-α, IL-6, IL-1β, and IL-10 after JQ1 treatment in M1 macrophages. As the result of mRNA expression in macrophages (Figure S2), JQ1 dose-dependently inhibited inflammatory markers and induced anti-inflammatory markers. To confirm the anti-inflammatory effects of each experimental group, IFRep gel only (+IFRep gel) and JQ1-loaded IFRep gels (+IFRep gel_JQ1), and JQ1-loaded non-IFRep gels (+NIFRep gel_JQ1) were treated with M1 macrophages. First, we tested the mechanism underlying the anti-inflammatory effect of BRD4 inhibition in macrophages. Nrf2 activation in macrophages and consequent expression of antioxidant and anti-inflammatory factors were analyzed. Exposure of M1 macrophages to JQ1-loaded IFRep gels activated the transcription of antioxidation-related enzymes, including heme oxygenase-1, NADPH quinine oxidoreductase-1, and superoxide dismutase by inducing translocation of Nrf2 into the cell nucleus (Figure 6a–c). Additionally, the level of reactive oxygen species (ROS) expressed in the inflammatory environment was significantly suppressed in + IFRep gel_JQ1-treated macrophages (Figure 6d,e).[32,33] As a result, mRNA expression of the inflammatory markers TNF-α, IL-6, and IL-1β, and CD197 was significantly inhibited in the + IFRep gel_JQ1-treated group compared to that in the + IFRep gel- and +NIFRep gel_JQ1-treated groups (Figure 6f). In the +NIFRep gel_JQ1-treated group, relatively low inhibition of inflammation effects was observed because of the non-responsiveness of NIFRep gel to cathepsins, resulting in a diffusion mechanism to deliver a smaller amount of JQ1 to macrophages. In ELISA, TNF-α and IL-1β levels showed the greatest decrease after treatment with JQ1-loaded IFRep gels (Figure 6g). The Nrf2 signal blocks the transcription of inflammatory cytokines and inhibits the inflammatory response by increasing the expression of antioxidant genes.[34−36] Taken together, these results indicate that the IFRep gel-mediating BRD4 inhibition can effectively inhibit inflammatory responses in macrophages by regulating Nrf2 signaling pathways (Figure 6h).

Accelerated Wound Healing *In Vivo* via IFRep Gel Loaded with a BRD4 Inhibitor. After confirming the function of the IFRep gel in drug release in response to inflammation and the potential of the IFRep gel in epigenetic modulation in inflammatory macrophages for anti-inflammation with a BRD4 inhibitor, we further directly tested the ability of IFRep gels to control on-demand epigenetic therapy *in vivo*. For this, a full-thickness wound of the mouse was treated with the IFRep gel, JQ1-loaded IFRep hydrogel (IFRep gel_JQ1), and JQ1-loaded non-IFRep hydrogel (NIFRep gel_JQ1) for 14 days. The wound closure was accelerated in the IFRep gel-treated group (32.30 ± 9.99%) compared to in the saline-treated group (47.39 ± 3.12%), which was the negative control. This result is supported by those of previous studies demonstrating the effectiveness of alginate hydrogel in wound closure by maintaining a moist environment and absorbing excessive wound fluid.[37,38] Additionally, IFRep gel_JQ1-treated group (17.27 ± 3.79%) enhanced the wound closure rate compared with the IFRep gel only-treated group (Figure 7a,b). In particular, IFRep gel_JQ1 exhibited the most significant wound closure on day 14 than NIFRep gel_JQ1-treated group (31.19 ± 6.50%). The histological analysis with H&E staining indicated the greatest increases in re-epithelialization and total dermal thickness following IFRep gel_JQ1 treatment (Figure 7c,e). Furthermore, complete restoration of the epidermis was investigated with IFRep gel_JQ1 using immunofluorescence staining of the cytokeratin 10 marker to detect the keratinocyte distribution in the wound site (Figure 7g). The IFRep gel_JQ1 induced the highest level of mature collagen deposition, as indicated by the red color of Herovici staining in the wound bed (Figure 7d,f). Among the experimental groups, only IFRep gel_JQ1-treated group showed the most similar thickness of the epidermis, dermis formation, and distribution of mature collagen to normal skin tissue. Finally, to assess the local immunomodulation efficacy of the JQ1-loaded IFRep gel, we evaluated the expression of pro- and anti-inflammatory markers in all groups (Figure 7h). The overlapping staining of the inflammatory marker iNOS and macrophage marker CD11b in M1 macrophages was dramatically decreased on day 14 in the IFRep gel_JQ1 group. The overlapping staining of the anti-inflammatory markers CD206 and CD11b in M2 macrophages was increased in the IFRep gel_JQ1 group compared to in the IFRep gel and NIFRep gel_JQ1 groups. In addition, inflammatory gene levels were mostly suppressed and anti-inflammatory gene levels were significantly upregulated in the IFRep gel_JQ1 group (Figure 7i). Collectively, the IFRep gel loaded with the BRD4 inhibitor enhanced the therapeutic efficacy by conferring on-demand epigenetic control according to the state of inflammation, as indicated by accelerated wound healing

https://doi.org/10.1021/acsami.1c20394
ACS Appl. Mater. Interfaces XXXX, XXX, XXX−XXX

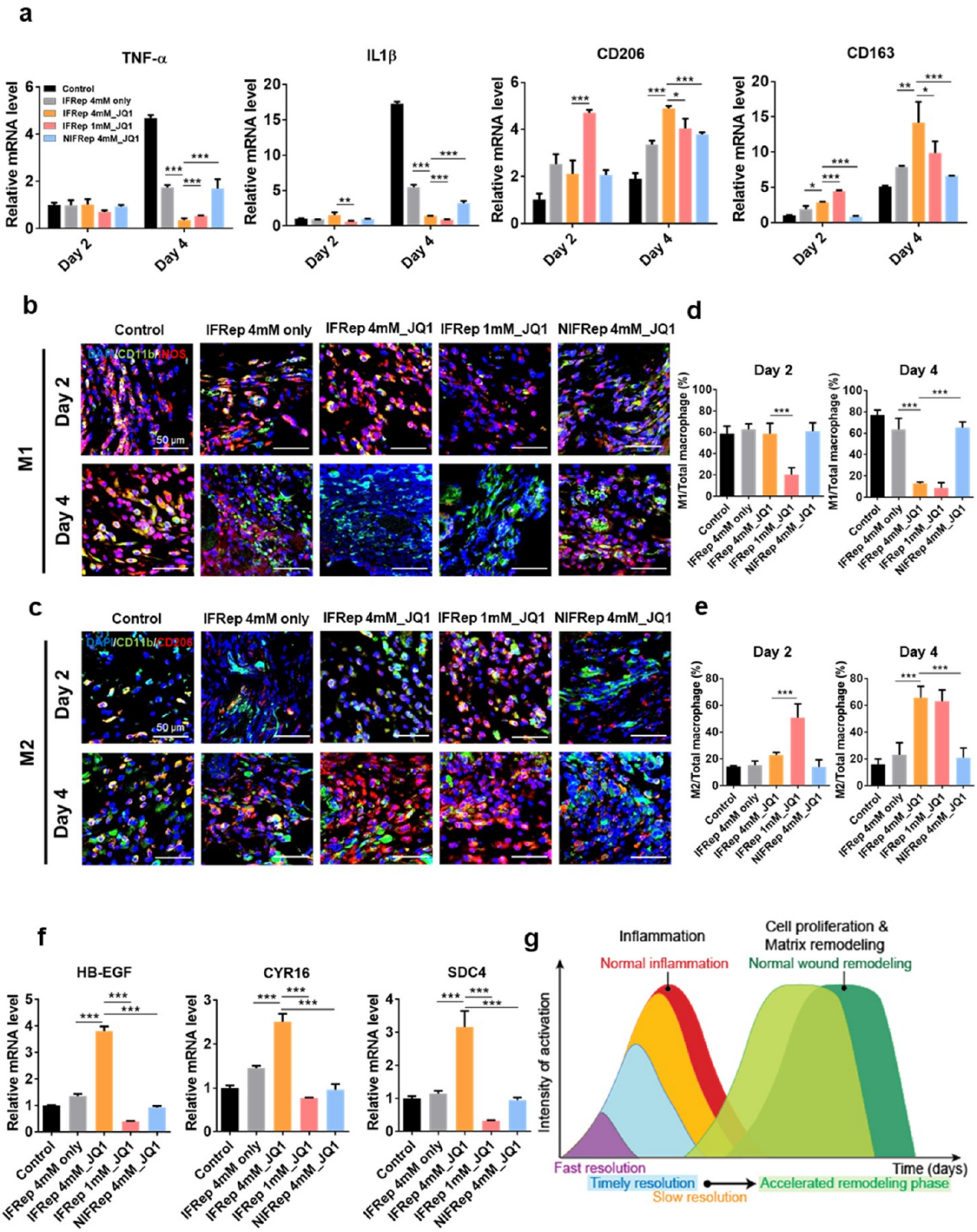

Figure 8. Timely resolution of inflammation with BRD4-loaded inflammation-responsive hydrogel drives keratinocyte activation in wound healing. (a) mRNA level of inflammatory and anti-inflammatory markers on days 2 and 4. (b, c) Immunofluorescence staining of M1 and M2 markers. (d,e) Quantification of M1 and M2 population in immunofluorescence images on days 2 and 4. (f) mRNA level of keratinocyte activation markers on day 4. (g) Schematic illustration of accelerated wound remodeling phase via timely resolution of inflammation phase in the wound injury. Data are presented as mean ± SD, $n = 3$ (*$p < 0.1$, **$p < 0.01$, ***$p < 0.001$).

compared to nonresponsive BRD4 inhibition via the NIFRep gel.

On-Demand BRD Inhibition Using the Responsive Hydrogel Determined Effective Wound Recovery by Controlling the Early Inflammatory Phase and Keratinocyte Activation *In Vivo*. To investigate the underlying mechanism associated with the enhanced therapeutic efficacy of on-demand BRD inhibition corresponding to the state of inflammation, we further tested the effect of responsive drug release on keratinocyte activation in the early inflammatory phase. Various JQ1-loaded hydrogels were applied after wound formation. After 2 days, the levels of inflammatory markers rapidly decreased by immediate drug release after treatment in the IFRep 1mM_JQ1 group, whereas inflammatory response was maintained in the other groups compared to the control group (Figure 8a). Inflammatory marker levels were

https://doi.org/10.1021/acsami.1c20394
ACS Appl. Mater. Interfaces XXXX, XXX, XXX−XXX

significantly suppressed in the IFRep 4mM_JQ1 group, and the inflammatory response was enhanced in the control, gel-only, and NIFRep 4mM_JQ1 groups after day 4 compared with those after day 2. Moreover, upregulation of anti-inflammatory marker expression was highest in IFRep 1mM_JQ1 on day 2, whereas IFRep 4mM_JQ1 was highest on day 4. Additionally, NIFRep 4mM_JQ1 exhibited no significant inflammatory suppression between days 2 and 4. Immunofluorescence analysis showed that the M1 marker (CD11b+iNOS+ positive cells) level was promptly suppressed and the M2 marker (CD11b+CD206 + positive cells) level was increased in the IFRep 1mM_JQ1 group on day 2 (Figure 8b–e). However, these effects were observed on day 4 in the IFRep 4mM_JQ1 group, which is consistent with the results of mRNA expression analysis. Therefore, the IFRep 4mM-JQ1 group showed a proactive M1–M2 transition, in which the inflammatory response was increased and then appropriately resolved. Previous studies also demonstrated that disruption of timely transition of M1–M2 macrophages by excessive inhibition of M1 macrophages after tissue injury prevents tissue regeneration.[39−41] Additionally, we further investigated the correlation between inflammation and keratinocyte activation. HB-EGF, CYR61, and SDC are key activation markers of keratinocytes in wound healing because they promote keratinocyte migration and re-epithelialization. Interestingly, only IFRep 4mM_JQ1 activated keratinocytes for wound healing on day 4 (Figure 8f). As expected, either a nonresponsive or immediate drug release could not activate keratinocytes for reepithelialization on day 4, supporting the therapeutic value of on-demand BRD4 inhibition via the IFRep hydrogels for effective wound recovery. A recent study demonstrated that a BRD4 inhibitor regulates keratinocyte plasticity and that low-dose BRD4 inhibition contributes to effective keratinocyte activation.[42] As proliferation is an important step promoting keratinocyte migration and proliferation after inflammation resolution in the wound healing process, rapidly advancing to the proliferation phase after inflammation resolution can be regarded as an important aspect of promoting tissue regeneration.[43] Our *in vivo* results were consistent with the previous wound healing studies using drug-loaded hydrogel regarding wound closure rate, epidermis formation, and regenerated dermis tissue thickness. In the previous study, Wang et al. demonstrated that a hyaluronic acid hydrogel encapsulating peptide drug effectively enhanced acute mouse wound healing and showed almost 100% healing efficacy after 20-day treatment.[44] As another example of wound healing using hydrogel-containing drug, Zheng *et al.* developed cannabidiol (CBD)-containing alginate hydrogel, which shows antioxidant and anti-inflammatory effects. In an acute rat wound model, CBD-containing alginate hydrogel showed almost 90% dermis restoration after 14-day treatment.[45] These previous studies demonstrated that each of their specialized systems is effective to wound healing. In contrast to those previous studies only showing enhanced wound healing results, we considered more detailed proof of the relation between modulation of macrophage and wound healing. Furthermore, for detailed proof, we investigated keratinocyte activation implying a regulator for accelerating the wound healing process. Collectively, these results indicate that IFRep 4mM_JQ1 accelerated wound healing as a transition from the inflammation to the proliferation phase by controlling acute inflammation for effective wound regeneration (Figure 8g).

The engineered hydrogel in this study showed timely control of BRD inhibition for the desirable M1–M2 macrophage transition for effective wound healing. Accordingly, the IFRep gel is capable of modulating epigenetic reprogramming, demonstrating its potential as a therapeutic strategy for favorable immunomodulation to treat different types of inflammatory diseases with different combinations of drugs. Ultimately, the system developed in this study may have wide biomedical applications in anti-inflammatory therapy for inflammatory diseases such as bowel disease, rheumatoid arthritis, asthma, and atherosclerosis.

CONCLUSIONS

We developed a hydrogel responsive to cathepsins that are overexpressed in inflammatory environments for local anti-inflammatory therapy. The IFRep gel showed controlled drug release in the presence of various cathepsins and inflammation. Additionally, the loaded BRD4 inhibitor was rapidly released from the IFRep hydrogel in response to the inflammatory environment and exerted anti-inflammatory effects. As the delivered epigenetic drug, the BRD4 inhibitor effectively suppressed inflammatory macrophages via Nrf2 activation, resulting in increased transcription of antioxidant genes. *In vitro* experiments demonstrated that the IFRep gel was biocompatible and reliable for active drug delivery in an inflammatory environment. The wound healing *in vivo* results showed that the BRD4 inhibitor from the IFRep gel induced appropriate resolution of inflammation and enhanced tissue regeneration. Particularly, compared with nonresponsive hydrogels, active immunomodulation using IFRep gels had significant advantages in terms of effective BRD4 inhibitor delivery and wound healing. The IFRep gel exhibited effective drug delivery for anti-inflammation therapy and high potential for wound healing with immunomodulation. This approach is a promising therapeutic strategy for favorable immunomodulation to treat different types of inflammatory diseases using different combinations of drugs.

EXPERIMENTAL SECTION

Fabrication of Norbornene-Conjugated Alginate (Nor_Alg). Alginate (PRONOVA UP) was dissolved in MES buffer (pH 6.5) at a concentration of 1 wt %. 1-Ethyl-3-(3-dimethylaminopropyl) carbodiimide hydrochloride (EDC) (40 mM) and *N*-hydroxysuccinimide (NHS) (60 mM) were dissolved in the alginate solution for 30 min. Then, 20 mM 5-norbornene-2-methylamine was added and the reaction was kept at room temperature for 24 h. After the reaction was over, the solution was transferred to a 25 kDa MWCO dialysis tube and dialyzed with NaCl solutions of 100, 50, 25, and 0 mM in deionized water (DI) sequentially. The dialysate was changed every 10 h for 3 days. Norbornene-conjugated alginate (Nor_Alg) solution was sterilized with a 0.22 μm filter and freeze-dried for 2 days. The successful modification of alginate was confirmed via ^{1}H-NMR measurement (sample concentration at 2 wt % in deuterium oxide).

Preparation of Peptide Cross-Linked Nor_Alg Gel (IFRep Gel). Nor_Alg (2 wt %) was dissolved in DI water, and 0.5% Irgacure was added to a solution. Cathepsins-cleavable peptide cross-linker CARLRC (MW: 720.35, purity: 98%, Peptron) was designed based on a previous publication.[46] Nor_Alg with Irgacure was added in a mold, then cathepsins-cleavable cross-linker was added with various concentrations of 1, 2, and 4 mM. The mixture of solutions was exposed to UV light (365 nm, 10 mW/cm^2) for 10 min. Additionally, poly(ethylene glycol), A,Ω-bis(thiol)-terminated cross-linker (Polymer Source, Inc. #P20223A-EG2SH, MW: 460) was used to fabricate non-inflammation-responsive hydrogel (NIFRep gel) in the same concentration as the cathepsins-cleavable cross-linker.

https://doi.org/10.1021/acsami.1c20394
ACS Appl. Mater. Interfaces XXXX, XXX, XXX−XXX

Mechanical Property. The rheology of IFRep gel was analyzed using a rheometer (Anton Paar). The measurements were performed at an oscillating frequency from 0.1 to 100 rad s^{-1} at 0.1% strain at room temperature. The storage modulus (G') and loss modulus (G'') were calculated by the software of instrument. Also, the stiffness of IFRep gel was analyzed using Instron 5900 (Instron Corporation). The hydrogels were compressed to 20% of the height, the stress−strain curve was measured, and Young's modulus was obtained with the slope of the linear area in the stress−strain curve.

SEM Imaging. The lyophilized hydrogel was added to liquid nitrogen for a clear cross section of the sample. The cutting sample was placed on carbon tape, and the surface was coated with platinum. The prepared samples were visualized with scanning electron microscopy (SEM).

Swelling Property. For hydrogel swelling property analysis, the IFRep gels were lyophilized and weighed as the initial dry weight of the sample (W_0) and then placed in PBS at 37 °C. Swollen samples were weighed at the time point (W_t), and the swelling ratio was calculated via the following equation:

$$\text{swelling ratio}(\%) = W_0 - W_t/W_0 \times 100$$

Drug Loading and Release Profile from IFRep Gel. Dextran (MW 4 kDa) and Cy7-CA (a model compound for small molecules) were loaded in the IFRep gel for cargo release profile under various conditions. Dextran- and Cy7-CA-loaded IFRep gels were placed in 24 transwell inserts and incubated in PBS, media, M0- and M1-like macrophage-conditioned media at 37 °C. The inserts were transferred to a new 24-well plate, and the fluorescence intensity was visualized with *in vivo* imaging system (IVIS) at the time point. Also, (+)-JQ1 ((6S)-4-(4-chlorophenyl)-2,3,9-trimethyl-6*H*-thieno[3,2-*f*][1,2,4]-triazolo[4,3-*a*][1,4]diazepine-6-acetic acid, 1,1-dimethylethyl ester, Selleckchem)-loaded IFRep gels were incubated in PBS, media, M0- and M1-like macrophage-conditioned media at 37 °C. The supernatants were collected at the time point and quantified via ultraviolet (UV) absorbance at 254 nm. Also, (+)-JQ1 release profile test was performed under different cathepsins in PBS 37 °C. Activated cathepsins L, S, and B were added at a concentration of 100 ng/ml, respectively, and the supernatants were collected for UV absorbance measurement. Cathepsins were added at every time point. Additionally, E-64 inhibitor was added for cathepsins inhibition in PBS with cathepsins L, S, and B.

Cell Culture. Human monocyte cell line THP-1 was purchased from American Type Culture Collection (ATCC) and cultured in Roswell Park Memorial Institute Medium (RPMI 1640) supplemented with 10% fetal bovine serum (FBS) and 1% penicillin/streptomycin (PS). Also, fibroblast (NIH3T3) was cultured in Dulbecco's modified Eagle's medium (DMEM) supplemented with 10% FBS and 1% PS. The cells were incubated in a humid atmosphere with 5% CO_2 at 37 °C.

Cytotoxicity Assay. The cytotoxicity of IFRep gels was analyzed using Cell Counting Kit-8 assay (CCK-8, Dojindo). Fibroblasts and THP-1 were seeded in 24-well plates and cultured with IFRep gels placed in the 24 transwell insert. After incubation with IFRep gels, the cells were washed with PBS and immersed in free media with 10% CCK-8 solution for 2 h at 37 °C. The supernatant was collected and measured at 450 nm absorbance using a microplate reader.

THP-1 Polarization. For differentiation of monocytes to macrophages, THP-1 cells were cultured with 50 ng/mL phorbol 12-myristate 13-acetate (PMA, Sigma #P1585) for 2 days. M0 macrophages differentiated M1-like macrophages with 100 ng/mL LPS (Sigma, #L2630) and 20 ng/mL hIFN-γ (PEPROTECH, #300-02) in a complete medium for 2 days. As shown in Figure S1, the differentiation was confirmed by M1 and M2 biomarkers, CD197 and DC-SIGN, respectively, using both qPCR and flow cytometry.

Protease Array. The conditioned media of M0- and M1-like macrophages were collected after 1-day incubation and used for the protease array experiment. The procedure was performed according to the manufacturer's instructions (Abcam #ARY021B).

Cathepsin Activity Assay. For confirmation of secreted cathepsins from M0- and M1-like macrophages, the conditioned medium was harvested after 1-day incubation of M0- and M1-like macrophages in media. To analyze the activity of cathepsins L and B, fluorescence-based assay kits (Biovision) were used. The procedure was performed according to the manufacturer's instructions. The fluorescence intensity of samples was measured with a fluorescence plate reader at 400/505 nm (Ex/Em).

Quantitative Real-Time Polymerase Chain Reaction (Real-Time PCR). The gene expression of cathepsins (cathepsins L, S, B, K, and D) and inflammatory markers, including TNF-α, IL-6, IL1β, and IL-10, was analyzed by real-time PCR assay. M1-like macrophages were cultured with JQ1-loaded IFRep gels for 48 h and mRNA in macrophages was isolated using RNeasy Mini Kit (QIAGEN), and synthesized to cDNA using a SuperScript IV VILO Master Mix (Invitrogen). Also, gene-level expression was performed with an SYBR Premix Ex Taq (Takara) according to the manufacturer's instruction. The sequences of primers were GAPDH (forward 5′-CACCATTGGCAATGAGCGGTTC-3′, reverse 5′-AGGTCTTTGCGGATGTCCACGT-3′), Cathepsin L (forward 5′-GAAAGGCTACGTGACTCCTGTG-3′, reverse 5′- GTCTACCAGATTCTGCTCACTC-3), Cathepsin S (forward 5′-TGGATCACCACTGGCATCTCTG-3′, reverse 5′-GCTCCAGGTTGTGAAGCATCAC-3′), TNF-α (forward 5′-GTGCCTATGTCTCAGCCTCTTC-3′, reverse 5′-GCCATAGAACTGATGAGAGGGA-3′), Cathepsin B (forward 5′-GCTTCGATGCACGGGAACAATG-3′, reverse 5′-CATTGGTGTGGATGCAGATCCG-3′), Cathepsin K (forward 5′-GAGGCTTCTCTTGGTGTCCATAC-3′, reverse 5′-TTACTGCGGGAATGAGACAGGG-3′), Cathepsin D (forward 5′-GCAAACTGCTGGACATCGCTTG-3′, reverse 5′-GCCATAGTGGATGTCAAACGAGG-3′), TNF-α (forward 5′-GTGCCTATGTCTCAGCCTCTTC-3′, reverse 5′-GCCATAGAACTGATGAGAGGGA-3′), IL-6 (forward 5′-CTTCCATCCAGTTGCCTTCTTG-3′, reverse 5′-AATTAAGCCTCCGACTTGTGAAG-3′), IL1β (forward 5′-CCACAGACCTTCCAGGAGAATG-3′, reverse 5′-GTGCAGTTCAGTGATCGTACAGG-3′), and IL-10 (forward 5′-TCTCCGAGATGCCTTCAGCAGA-3′, reverse 5′- TCAGACAAGGCTTGGCAACCCA-3′). The expressed gene levels were normalized to GAPDH as the housekeeping gene, and the relative gene level was calculated by the $2^{-\triangle\triangle CT}$ method.

ROS Fluorescence Staining. After treatment of IFRep gel, JQ1-loaded IFRep gel, and JQ1-loaded NIFRep gel to M1-like macrophages for 48 h, the cells were washed with PBS and treated with 2′,7′-dichlorofluorescein (Sigma #D6665) solution at a final concentration of 10 μM. After incubation for 30 min, the cells were washed and imaged with a confocal microscope (Carl Zeiss).

Immunofluorescent Staining. After treatment of IFRep gel, JQ1-loaded IFRep gel, and JQ1-loaded NIFRep gel to M1-like macrophages for 48 h, immunofluorescence staining of Nrf2 was conducted. The cells were fixed with 4% paraformaldehyde for 30 min at room temperature and washed with PBS three times. Then, fixed cells were permeabilized with 0.1% Triton X-100 in PBS for 15 min and blocked with 3% bovine serum albumin (BSA) for 1 h at room temperature. Sequentially, the primary antibody of Nrf2 (Cell Signaling, #12721) in 3% BSA was treated and incubated overnight at 4 °C. The samples were washed with PBS three times and then treated with the second antibody Rabbit IgG (Invitrogen, #A21207) for 1 h at room temperature. After the incubation, PBS washing and DAPI staining were performed for 5 min. The immunostained section was observed by a confocal microscope (Carl Zeiss). For immunofluorescence staining of *in vivo* sectioned tissue, CD11b (Biolegend, #101201), iNOS (Millipore, #06-573), TNF-α (#ab183218), Cathepsin L (#ab133641), S (#sc-271619), B (#ab214428), and cytokeratin 10 (#ab76318) were used for primary antibodies and the secondary antibodies Rabbit IgG (Invitrogen, #A21207) and Goat anti-Mouse IgG (Invitrogen, #A11001) were used.

ELISA Assay. The supernatants of IFRep gel-, JQ1-loaded IFRep gel-, and JQ1-loaded NIFRep gel-treated M1-like macrophages (2 mL/10^6 cells) were collected and analyzed using TNF-α ELISA kit (R&D systems, #DTA00D) and IL1β DuoSet kit (R&D systems,

https://doi.org/10.1021/acsami.1c20394
ACS Appl. Mater. Interfaces XXXX, XXX, XXX−XXX

#DY201). The quantification of TNF-α and IL1β was measured by GloMax Discover Multimode Microplate Reader (Promega) at 450 nm.

***In Vivo* Full-Thickness Wound Model.** The animal study was approved by Korea Institute of Science and Technology (KIST-2020-046). All animal experiments were performed according to the International Guide for the Care and Use of Laboratory Animals. Balb/c mice (male, 6 weeks) were purchased from Orient Bio (Korea) and used after an acclimation period of 1 week. Before surgery, the mouse was anesthetized by isoflurane in oxygen, and the hair was removed using a clipper. After sterilization with an alcohol gauze, full-thickness wounds were made using an 8 mm biopsy punch on a dorsal skin (two wounds per mouse). The 0.5 mm thick silicon splinting ring was glued and sutured around the wound. The IFRep gel, JQ1-loaded IFRep gel, and JQ1-loaded NIFRep gels were applied to a wound area. Then, the wound area was covered with Tegaderm Film, and Coban bandage was attached sequentially. Moreover, for 14 days of wound healing *in vivo* study, 4 mM concentration of cross-linker was used and 1 mM concentration of cross-linked hydrogel was added for day 2 and 4 time point studies.

Histology. The harvested samples were fixed with 10% formalin and immersed in paraffin blocks. The tissue blocks were sectioned in 6−7 μm slices and deparaffinized and hydrated sequentially by treating xylene and ethanol solutions, respectively. The slices were stained with hematoxylin and eosin staining (H&E) and Herovici staining and observed with an optical microscope.

Statistical Analysis. All data were expressed as mean ± standard deviation, and each experiment was performed in triplicate for three separate experiments. Data were analyzed using a one-way analysis of variance (ANOVA) followed by Tukey's post hoc test or unpaired *t*-test in Prism. Statistical significance was $^{*}p < 0.05$, $^{**}p < 0.01$, and $^{***}p < 0.001$.

■ ASSOCIATED CONTENT

Supporting Information

The Supporting Information is available free of charge at https://pubs.acs.org/doi/10.1021/acsami.1c20394.

Additional details on the M1 macrophage polarization assay used *in vitro* by optical images, flow cytometry staining, and real-time PCR (Figure S1) and the anti-inflammatory effect of various JQ1 concentrations on the M1 inflammatory response by real-time PCR (Figure S2) (PDF)

■ AUTHOR INFORMATION

Corresponding Authors

Kangwon Lee − *Department of Applied Bioengineering, Graduate School of Convergence Science and Technology and Research Institute for Convergence Science, Seoul National University, Seoul 08826, Republic of Korea;* orcid.org/0000-0001-5745-313X; Email: kangwonlee@snu.ac.kr

Seung Ja Oh − *Center for Biomaterials, Biomedical Research Institute, Korea Institute of Science and Technology (KIST), Seoul 02792, Republic of Korea; Department of Biomedical Engineering, Korea University of Science and Technology (UST), Daejeon 34113, Republic of Korea;* orcid.org/0000-0002-4572-0656; Email: seungja.oh@kist.re.kr

Authors

Hyerim Kim − *Program in Nanoscience and Technology, Graduate School of Convergence Science and Technology, Seoul National University, Seoul 08826, Republic of Korea*

Yunji Joo − *Center for Biomaterials, Biomedical Research Institute, Korea Institute of Science and Technology (KIST), Seoul 02792, Republic of Korea; Department of Biomedical Engineering, Korea University of Science and Technology (UST), Daejeon 34113, Republic of Korea*

Yun-Min Kook − *Center for Biomaterials, Biomedical Research Institute, Korea Institute of Science and Technology (KIST), Seoul 02792, Republic of Korea*

Na Ly Tran − *Center for Biomaterials, Biomedical Research Institute, Korea Institute of Science and Technology (KIST), Seoul 02792, Republic of Korea; Department of Biomedical Engineering, Korea University of Science and Technology (UST), Daejeon 34113, Republic of Korea*

Sang-Heon Kim − *Center for Biomaterials, Biomedical Research Institute, Korea Institute of Science and Technology (KIST), Seoul 02792, Republic of Korea; Department of Biomedical Engineering, Korea University of Science and Technology (UST), Daejeon 34113, Republic of Korea*

Complete contact information is available at: https://pubs.acs.org/10.1021/acsami.1c20394

Notes

The authors declare no competing financial interest.

■ ACKNOWLEDGMENTS

This work was supported and funded by NRF (National Research Foundation) of Korea grant funded by the Korea government (2020R1C1C1009507) and the KIST Institutional Program to S.J.O. Also, this work was supported by a grant from Nano & Material Technology Development Program through NRF funded by the Ministry of Science and ICT (NRF-2017M3A7B4049850) to K.L. Finally, this work was supported by NRF Grant funded by the Korean Government (NRF-2017-Global Ph.D. Fellowship Program, 2017H1A2A1043981) to H.K.

■ REFERENCES

(1) Eming, S. A.; Wynn, T. A.; Martin, P. Inflammation and Metabolism in Tissue Repair and Regeneration. *Science* **2017**, *356*, 1026−1030.

(2) Eming, S. A.; Krieg, T.; Davidson, J. M. Inflammation in Wound Repair: Molecular and Cellular Mechanisms. *J. Invest. Dermatol.* **2007**, *127*, 514−525.

(3) Kim, H.; Wang, S. Y.; Kwak, G.; Yang, Y.; Kwon, I. C.; Kim, S. H. Exosome-Guided Phenotypic Switch of M1 to M2 Macrophages for Cutaneous Wound Healing. *Adv. Sci.* **2019**, *6*, No. 1900513.

(4) Raimondo, T. M.; Mooney, D. J. Functional Muscle Recovery With Nanoparticle-Directed M2 Macrophage Polarization in Mice. *Proc. Natl. Acad. Sci. U.S.A.* **2018**, *115*, 10648−10653.

(5) Dellacherie, M. O.; Seo, B. R.; Mooney, D. J. Macroscale Biomaterials Strategies for Local Immunomodulation. *Nat. Rev. Mater.* **2019**, *4*, 379−397.

(6) Saleh, B.; Dhaliwal, H. K.; Portillo-Lara, R.; Shirzaei Sani, E.; Abdi, R.; Amiji, M. M.; Annabi, N. Local Immunomodulation Using an Adhesive Hydrogel Loaded with miRNA-Laden Nanoparticles Promotes Wound Healing. *Small* **2019**, *15*, No. 1902232.

(7) Salehi, M.; Ehterami, A.; Farzamfar, S.; Vaez, A.; Ebrahimi-Barough, S. Accelerating Healing of Excisional Wound with Alginate Hydrogel Containing Naringenin in Rat Model. *Drug Delivery Transl. Res.* **2021**, *11*, 142−153.

(8) Zhang, S.; Liu, Y.; Zhang, X.; Zhu, D.; Qi, X.; Cao, X.; Fang, Y.; Che, Y.; Han, Z. C.; He, Z. X.; Han, Z.; Li, Z. Prostaglandin E2 Hydrogel Improves Cutaneous Wound Healing via M2 Macrophages Polarization. *Theranostics* **2018**, *8*, 5348−5361.

(9) Chen, H.; Cheng, R. Y.; Zhao, X.; Zhang, Y. H.; Tam, A.; Yan, Y. F.; Shen, H. K.; Zhang, Y. S.; Qi, J.; Feng, Y.; Liu, L.; Pan, G. Q.; Cui, W. G.; Deng, L. F. An Injectable Self-Healing Coordinative Hydrogel

with Antibacterial and Angiogenic Properties for Diabetic Skin Wound Repair. *NPG Asia Mater.* **2019**, *11*, No. 3.
(10) Hu, C.; Zhang, F. J.; Long, L. Y.; Kong, Q. S.; Luo, R. F.; Wang, Y. B. Dual-Responsive Injectable Hydrogels Encapsulating Drug-Loaded Micelles for On-Demand Antimicrobial Activity and Accelerated Wound Healing. *J. Controlled Release* **2020**, *324*, 204−217.
(11) Ninan, N.; Forget, A.; Shastri, V. P.; Voelcker, N. H.; Blencowe, A. Antibacterial and Anti-Inflammatory pH-Responsive Tannic Acid-Carboxylated Agarose Composite Hydrogels for Wound Healing. *Acs Appl. Mater. Interfaces* **2016**, *8*, 28511−28521.
(12) Joshi, N.; Yan, J.; Levy, S.; Bhagchandani, S.; Slaughter, K. V.; Sherman, N. E.; Amirault, J.; Wang, Y. F.; Riegel, L.; He, X. Y.; Rui, T. S.; Valic, M.; Vemula, P. K.; Miranda, O. R.; Levy, O.; Gravallese, E. M.; Aliprantis, A. O.; Ermann, J.; Karp, J. M. Towards an Arthritis Flare-Responsive Drug Delivery System. *Nat. Commun.* **2018**, *9*, No. 1275.
(13) Zhang, S. F.; Ermann, J.; Succi, M. D.; Zhou, A.; Hamilton, M. J.; Cao, B. N.; Korzenik, J. R.; Glickman, J. N.; Vemula, P. K.; Glimcher, L. H.; Traverso, G.; Langer, R.; Karp, J. M. An Inflammation-Targeting Hydrogel for Local Drug Delivery in Inflammatory Bowel Disease. *Sci. Transl. Med.* **2015**, *7*, No. 300ra128.
(14) Chen, L. B.; Yan, D.; Wu, N. A. X.; Yao, Q. K.; Sun, H.; Pang, Y.; Fu, Y. Injectable Bio-Responsive Hydrogel for Therapy of Inflammation Related Eyelid Diseases. *Bioact. Mater.* **2021**, *6*, 3062−3073.
(15) Alvarez, M. M.; Liu, J. C.; Trujillo-de Santiago, G.; Cha, B. H.; Vishwakarma, A.; Ghaemmaghami, A. M.; Khademhosseini, A. Delivery Strategies to Control Inflammatory Response: Modulating M1-M2 Polarization in Tissue Engineering Applications. *J. Controlled Release* **2016**, *240*, 349−363.
(16) Spiller, K. L.; Koh, T. J. Macrophage-Based Therapeutic Strategies in Regenerative Medicine. *Adv. Drug Delivery Rev.* **2017**, *122*, 74−83.
(17) Hesketh, M.; Sahin, K. B.; West, Z. E.; Murray, R. Z. Macrophage Phenotypes Regulate Scar Formation and Chronic Wound Healing. *Int. J. Mol. Sci.* **2017**, *18*, 1545.
(18) Ivashkiv, L. B. Epigenetic Regulation of Macrophage Polarization and Function. *Trends Immunol.* **2013**, *34*, 216−223.
(19) Takeuch, O.; Akira, S. Epigenetic Control of Macrophage Polarization. *Eur. J. Immunol.* **2011**, *41*, 2490−2493.
(20) Wang, J. L.; Chen, J. X.; Jin, H. M.; Lin, D. D.; Chen, Y.; Chen, X. M.; Wang, B.; Hu, S. L.; Wu, Y.; Wu, Y. S.; Zhou, Y. F.; Tian, N. F.; Gao, W. Y.; Wang, X. Y.; Zhang, X. L. BRD4 Inhibition Attenuates Inflammatory Response in Microglia and Facilitates Recovery after Spinal Cord Injury in Rats. *J. Cell. Mol. Med.* **2019**, *23*, 3214−3223.
(21) Belkina, A. C.; Nikolajczyk, B. S.; Denis, G. V. BET Protein Function is Required for Inflammation: Brd2 Genetic Disruption and BET Inhibitor JQ1 Impair Mouse Macrophage Inflammatory Responses. *J. Immunol.* **2013**, *190*, 3670−3678.
(22) Cramer, S. A.; Adjei, I. M.; Labhasetwar, V. Advancements in the Delivery of Epigenetic Drugs. *Expert Opin. Drug Delivery* **2015**, *12*, 1501−1512.
(23) Mitchell, M. J.; Billingsley, M. M.; Haley, R. M.; Wechsler, M. E.; Peppas, N. A.; Langer, R. Engineering Precision Nanoparticles for Drug Delivery. *Nat. Rev. Drug Discovery* **2021**, *20*, 101−124.
(24) Reiser, J.; Adair, B.; Reinheckel, T. Specialized Roles for Cysteine Cathepsins in Health and Disease. *J. Clin. Invest.* **2010**, *120*, 3421−3431.
(25) Vidak, E.; Javorsek, U.; Vizovisek, M.; Turk, B. Cysteine Cathepsins and Their Extracellular Roles: Shaping the Microenvironment. *Cells* **2019**, *8*, 264.
(26) Ooi, H. W.; Mota, C.; ten Cate, A. T.; Calore, A.; Moroni, L.; Baker, M. B. Thiol-Ene Alginate Hydrogels as Versatile Bioinks for Bioprinting. *Biomacromolecules* **2018**, *19*, 3390−3400.
(27) Lueckgen, A.; Garske, D. S.; Ellinghaus, A.; Desai, R. M.; Stafford, A. G.; Mooney, D. J.; Duda, G. N.; Cipitria, A. Hydrolytically-Degradable Click-Crosslinked Alginate Hydrogels. *Biomaterials* **2018**, *181*, 189−198.
(28) Desai, R. M.; Koshy, S. T.; Hilderbrand, S. A.; Mooney, D. J.; Joshi, N. S. Versatile Click Alginate Hydrogels Crosslinked cia Tetrazine-Norbornene Chemistry. *Biomaterials* **2015**, *50*, 30−37.
(29) Hoyle, C. E.; Bowman, C. N. Thiol-Ene Click Chemistry. *Angew. Chem., Int. Ed.* **2010**, *49*, 1540−1573.
(30) Park, C. G.; Hartl, C. A.; Schmid, D.; Carmona, E. M.; Kim, H. J.; Goldberg, M. S. Extended Release of Perioperative Immunotherapy Prevents Tumor Recurrence and Eliminates Metastases. *Sci. Transl. Med.* **2018**, *10*, No. eaar1916.
(31) Heerboth, S.; Lapinska, K.; Snyder, N.; Leary, M.; Rollinson, S.; Sarkar, S. Use of Epigenetic Drugs in Disease: An Overview. *Genet. Epigenet.* **2014**, *6*, No. GEG.S12270.
(32) Mittal, M.; Siddiqui, M. R.; Tran, K.; Reddy, S. P.; Malik, A. B. Reactive Oxygen Species in Inflammation and Tissue Injury. *Antioxid. Redox Signaling* **2014**, *20*, 1126−1167.
(33) Ferreira, I.; Silva, A.; Martins, J. D.; Neves, B. M.; Cruz, M. T. Nature and Kinetics of Redox Imbalance Triggered by Respiratory and Skin Chemical Sensitizers on the Human Monocytic Cell Line THP-1. *Redox. Biol.* **2018**, *16*, 75−86.
(34) Kobayashi, E. H.; Suzuki, T.; Funayama, R.; Nagashima, T.; Hayashi, M.; Sekine, H.; Tanaka, N.; Moriguchi, T.; Motohashi, H.; Nakayama, K.; Yamamoto, M. Nrf2 Suppresses Macrophage Inflammatory Response by Blocking Proinflammatory Cytokine Transcription. *Nat. Commun.* **2016**, *7*, No. 11624.
(35) Michaeloudes, C.; Mercado, N.; Clarke, C.; Bhavsar, P. K.; Adcock, I. M.; Barnes, P. J.; Chung, K. F. Bromodomain and Extraterminal Proteins Suppress NF-E2-Related Factor 2-Mediated Antioxidant Gene Expression. *J. Immunol.* **2014**, *192*, 4913−4920.
(36) Oh, Y. S.; Jun, H. S. Effects of Glucagon-Like Peptide-1 on Oxidative Stress and Nrf2 Signaling. *Int. J. Mol. Sci.* **2018**, *19*, No. 26.
(37) Gao, L.; Zhou, Y. L.; Peng, J. L.; Xu, C.; Xu, Q.; Xing, M.; Chang, J. A Novel Dual-Adhesive and Bioactive Hydrogel Activated by Bioglass for Wound Healing. *NPG Asia Mater.* **2019**, *11*, No. 66.
(38) Aderibigbe, B. A.; Buyana, B. Alginate in Wound Dressings. *Pharmaceutics* **2018**, *10*, 42.
(39) Zheng, Z. W.; Chen, Y. H.; Wu, D. Y.; Wang, J. B.; Lv, M. M.; Wang, X. S.; Sun, J.; Zhang, Z. Y. Development of an Accurate and Proactive Immunomodulatory Strategy to Improve Bone Substitute Material-Mediated Osteogenesis and Angiogenesis. *Theranostics* **2018**, *8*, 5482−5500.
(40) Li, T.; Peng, M. Z.; Yang, Z. Z.; Zhou, X. J.; Deng, Y.; Jiang, C.; Xiao, M.; Wang, J. W. 3D-Printed IFN-Gamma-Loading Calcium Silicate-Beta-Tricalcium Phosphate Scaffold Sequentially Activates M1 and M2 Polarization of Macrophages to Promote Vascularization of Tissue Engineering Bone. *Acta Biomater.* **2018**, *71*, 96−107.
(41) O'Brien, E. M.; Risser, G. E.; Spiller, K. L. Sequential Drug Delivery to Modulate Macrophage Behavior and Enhance Implant Integration. *Adv. Drug Delivery Rev.* **2019**, *149−150*, 85−94.
(42) Schutzius, G.; Kolter, C.; Bergling, S.; Tortelli, F.; Fuchs, F.; Renner, S.; Guagnano, V.; Cotesta, S.; Rueeger, H.; Faller, M.; Bouchez, L.; Salathe, A.; Nigsch, F.; Richards, S. M.; Louis, M.; Gruber, V.; Aebi, A.; Turner, J.; Grandjean, F.; Li, J.; Dimitri, C.; Thomas, J. R.; Schirle, M.; Blank, J.; Drueckes, P.; Vaupel, A.; Tiedt, R.; Manley, P. W.; Klopp, J.; Hemmig, R.; Zink, F.; Leroy, N.; Carbone, W.; Roma, G.; Keller, C. G.; Dales, N.; Beyerbach, A.; Zimmerlin, A.; Bonenfant, D.; Terranova, R.; Berwick, A.; Sahambi, S.; Reynolds, A.; Jennings, L. L.; Ruffner, H.; Tarsa, P.; Bouwmeester, T.; Driver, V.; Frederiksen, M.; Lohmann, F.; Kirkland, S. BET Bromodomain Inhibitors Regulate Keratinocyte Plasticity. *Nat. Chem. Biol.* **2021**, *17*, 280−290.
(43) Landén, N. X.; Li, D.; Stahle, M. Transition from Inflammation to Proliferation: A Critical Step During Wound Healing. *Cell. Mol. Life. Sci.* **2016**, *73*, 3861−3885.
(44) Wang, S. Y.; Kim, H.; Kwak, G.; Yoon, H. Y.; Jo, S. D.; Lee, J. E.; Cho, D.; Kwon, I. C.; Kim, S. H. Development of Biocompatible HA Hydrogels Embedded with a New Synthetic Peptide Promoting Cellular Migration for Advanced Wound Care Management. *Adv. Sci.* **2018**, *5*, No. 1800852.

https://doi.org/10.1021/acsami.1c20394
ACS Appl. Mater. Interfaces XXXX, XXX, XXX−XXX

(45) Zheng, Z.; Qi, J.; Hu, L.; Ouyang, D.; Wang, H.; Sun, Q.; Lin, L.; You, L.; Tang, B. A Cannabidiol-Containing Alginate Based Hydrogel as Novel Multifunctional Wound Dressing for Promoting Wound Healing. *Mater. Sci. Eng., C.* **2021**, No. 112560.
(46) Poreba, M.; Rut, W.; Vizovisek, M.; Groborz, K.; Kasperkiewicz, P.; Finlay, D.; Vuori, K.; Turk, D.; Turk, B.; Salvesen, G. S.; Drag, M. Selective Imaging of Cathepsin L in Breast Cancer by Fluorescent Activity-Based Probes. *Chem. Sci.* **2018**, *9*, 2113−2129.

https://doi.org/10.1021/acsami.1c20394
ACS Appl. Mater. Interfaces XXXX, XXX, XXX−XXX